

# 229Th-doped nonlinear optical crystals for compact solid-state clocks

H. W. T. Morgan,<sup>1,2</sup> R. Elwell,<sup>3</sup> J. E. S. Terhune,<sup>3</sup> H. B. Tran Tan,<sup>4,5</sup> U. C. Perera,<sup>4</sup> A. Derevianko,<sup>4</sup> A. N. Alexandrova,<sup>1</sup> and E. R. Hudson<sup>3,6,7</sup>

<sup>1</sup>Department of Chemistry and Biochemistry, University of California, Los Angeles, Los Angeles, CA 90095, USA

<sup>2</sup>Department of Chemistry, University of Manchester, Oxford Road, Manchester M13 9PL, UK

<sup>3</sup>Department of Physics and Astronomy, University of California, Los Angeles, CA 90095, USA

<sup>4</sup>Department of Physics, University of Nevada, Reno, Nevada 89557, USA

<sup>5</sup>Los Alamos National Laboratory, P.O. Box 1663, Los Alamos, New Mexico 87545, USA

<sup>6</sup>Challenge Institute for Quantum Computation, University of California Los Angeles, Los Angeles, CA, USA

<sup>7</sup>Center for Quantum Science and Engineering, University of California Los Angeles, Los Angeles, CA, USA

(Dated: 1 November 2024)

The recent laser excitation of the  $^{229}\text{Th}$  isomeric transition in a solid-state host opens the door for a portable solid-state nuclear optical clock. However, at present the vacuum-ultraviolet laser systems required for clock operation are not conducive to a fieldable form factor. Here, we propose a possible solution to this problem by using  $^{229}\text{Th}$ -doped nonlinear optical crystals, which would allow clock operation without a vacuum-ultraviolet laser system and without the need of maintaining the crystal under vacuum.

The unique properties of the  $^{229}\text{Th}$  nuclear isomeric state provide a laser accessible nuclear transition that can be driven even when doped into a high-bandgap solid<sup>1,2</sup>. This capability is expected to allow a number of groundbreaking experiments and applications, including the construction of a robust and portable optical nuclear clock<sup>3</sup>, exploration of nuclear super-radiance<sup>4</sup>, tests of fundamental physics<sup>2,5</sup>, and a new probe of the solid-state environment<sup>6,7</sup>.

The  $^{229}\text{Th}$  isomeric state was first identified in 1976 by  $\gamma$ -ray spectroscopy of decaying  $^{233}\text{U}$  and constrained to be  $< 100$  eV<sup>8</sup>. Over the ensuing decades, further experiments placed the isomer energy around 3.5 eV<sup>9</sup> and several, ultimately unsuccessful, attempts<sup>10,11</sup> were made to observe radiative decay of the isomeric state. Then in 2007-2009, an improved version of the original  $\gamma$ -ray spectroscopy experiment was performed and the isomer energy was revised to 7.8(5) eV<sup>12,13</sup>, placing the transition squarely in the vacuum ultraviolet (VUV) region of the spectrum and explaining why previous attempts at observing radiative decay, which were not performed in vacuum, failed. Since this measurement, there has been an intense effort to directly excite the nuclear transition with the first results reported earlier this year<sup>7,14</sup>. Thus, after nearly 50 years of work, the exciting applications of the  $^{229}\text{Th}$  isomeric transition are finally within reach.

Despite this important advance, challenges remain for realizing the aforementioned goals – particularly, realizing a portable nuclear clock system. The laser excitation of the isomeric state requires a rather difficult-to-achieve 148 nm laser. Thus far, experiments have employed either 4-wave mixing in xenon or high harmonic generation with a frequency comb to generate the requisite light and operated under high vacuum. While successful in exciting this transition, these rather bulky laser and vacuum systems are not particularly conducive to creating a portable nuclear clock.

Here, we detail two possible solutions<sup>15</sup> to this problem.

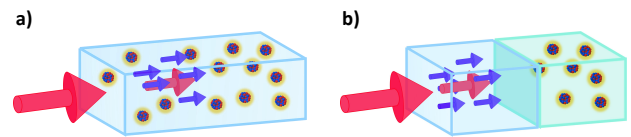


FIG. 1. A solid-state  $^{229}\text{Th}$  nuclear clock can be constructed without requiring vacuum operation by (a) doping  $^{229}\text{Th}$  directly into a nonlinear optical medium or (b) joining a  $^{229}\text{Th}$ -doped material directly to a nonlinear optical medium. This would allow, for example, the use of  $\sim 296.8$  nm light to excite the nuclear transition at  $\sim 148.4$  nm.

First, by doping  $^{229}\text{Th}$  *directly* into a nonlinear optical crystal, the requisite light can be generated and the nuclear transition interrogated *without* the need for vacuum operation. Second, by joining a nonlinear optical crystal directly to a  $^{229}\text{Th}$ -doped crystal, by e.g. optical contacting, the same capabilities can be realized. While in principle straightforward, this approach clearly requires a nonlinear optical crystal capable of generating 148 nm photons, which has not yet been demonstrated. Therefore, in what follows we first survey nonlinear optical materials that are potentially capable of generating light at 148 nm. We then present density functional theory (DFT) calculations of the geometry and electronic structure for these crystals when doped with thorium, we also discuss their suitability for joining with other crystalline hosts of  $^{229}\text{Th}$ , and conclude with a brief description of the use of these crystals in a solid-state clock.

## I. SURVEY OF POTENTIAL NONLINEAR OPTICAL CRYSTALS

The generation of higher energy photons from lower energy photons via nonlinear optical materials is an indispens-

able technique in modern optics. While ubiquitously applied throughout the visible and ultraviolet region (UV), efficient generation of photons at 148 nm using a solid-state nonlinear optical material has remained out of reach; the lowest wavelength generated by such methods is 149.8 nm<sup>16</sup>. This deficit of NLO materials for VUV operation stems from two facts. First, since the NLO material must be transparent to the generated light the material must have a large bandgap. This often precludes the use of crystalline structures containing oxygen, which have so far been the most commonly employed – e.g. BBO<sup>17</sup>. Second, because the indices of refraction of materials tend to increase strongly at VUV wavelengths, it is often difficult to ensure the phase matching condition can be met.

Nonetheless, there has been a concerted, if small, effort to develop NLO materials capable of generating VUV light<sup>18</sup>. Of the available materials, though fragile,  $\text{KBe}_2\text{BO}_3\text{F}_2$  (KBBF) has seen the most development and use. More recently, the material  $\gamma\text{-Be}_2\text{BO}_3\text{F}$  ( $\gamma$ -BBF) has been developed in hopes of solving the layering problem of KBBF<sup>19</sup>. This material is expected to be capable of SHG via Type I phase matching down to a wavelength of 146 nm<sup>19</sup>.

Apart from the BBF family, another promising approach is to use quasi-phase matching in periodically-poled, ferroelectric  $\text{BaMgF}_4$  and  $\text{BaZnF}_4$  crystals.  $\text{BaMgF}_4$  crystals are transparent to  $< 140$  nm, straightforward to pole, and appear stable under VUV illumination<sup>20,21</sup>.  $\text{BaZnF}_4$  is less studied than  $\text{BaMgF}_4$ , but similar properties appear possible<sup>22</sup>.

Thus, while other materials likely exist, the three most promising crystals at present for NLO generation of 148 nm light appear to be  $\gamma\text{-Be}_2\text{BO}_3\text{F}$ ,  $\text{BaMgF}_4$ , and  $\text{BaZnF}_4$ . Therefore, in what follows we study the possible configurations for <sup>229</sup>Th doped into  $\text{BaMgF}_4$  and  $\text{BaZnF}_4$ , as well as the resulting electronic structure, to ascertain their feasibility for use in a nuclear clock where a single crystal is used both to generate the requisite VUV light and host the thorium nuclei. We leave the case of  $\gamma\text{-Be}_2\text{BO}_3\text{F}$  for future work.

## II. DFT CALCULATIONS

### A. $\text{BaMgF}_4$

DFT is a powerful tool for studying point defects in crystalline hosts because of its high accuracy-to-cost balance, and it has been used in the development of a <sup>229</sup>Th crystal clock both to assess potential host crystals and to study the properties of thorium defects in thorium-free hosts<sup>7,23–25</sup>. Here we use DFT to investigate the structural and electronic properties of thorium defects in  $\text{BaMgF}_4$  to determine its potential as a clock material. We first optimized the structure of  $\text{BaMgF}_4$  ( $Cmc2_1$ ), shown in Figure 2(a). The lattice parameters are overestimated by 0–2% compared to the experimental crystal structure, as is typical for GGA functionals.<sup>26</sup> We then computed the density of states (DOS) using the MBJ functional, shown in Figure 2(b). The computed band gap is 10.03 eV, well above the <sup>229</sup>Th nuclear transition energy and in good agreement with a previous absorption edge measurement of 9.92 eV.<sup>27</sup> Superior methods for computing band gaps, such

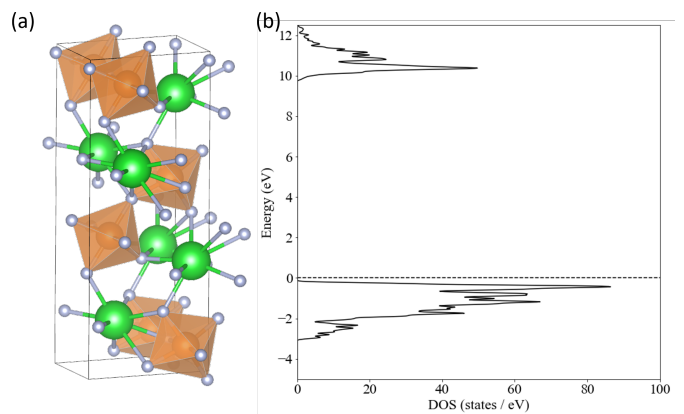


FIG. 2. (a) Unit cell of  $\text{BaMgF}_4$ . Ba is shown in green, Mg in orange, and F in light grey. (b) Total density of states (DOS) of  $\text{BaMgF}_4$ .

as GW methods or hybrid DFT functionals, may be feasible for small unit cells of pure materials but they are not practical on defect supercells. Thus, we compute the band gap and DOS with MBJ which is accurate and still affordable for large supercells<sup>7,28,29</sup>. These results show that our DFT model performs well on  $\text{BaMgF}_4$  and that this material is a good candidate clock material.

Having studied pure  $\text{BaMgF}_4$  we move to thorium defects. We begin our search for defect structures with the assumptions that thorium is in the +4 oxidation state, as is typical for halides and oxides, and that  $\text{Th}^{4+}$  replaces a  $\text{Ba}^{2+}$  in the lattice due to the higher coordination number of the  $\text{Ba}^{2+}$  site in  $\text{BaMgF}_4$ . This defect, denoted  $\text{Th}_{\text{Ba}}^{2+}$ , has a 2+ charge and so must be compensated by another defect with a net 2- charge. We have considered three possible identities for this defect: a barium vacancy,  $\text{V}_{\text{Ba}}^{2-}$ ; a magnesium vacancy,  $\text{V}_{\text{Mg}}^{2-}$ ; and a pair of fluoride interstitials,  $2\text{F}_i^-$ . In all cases we assume that the defect pairs are localized together, i.e. that the cation vacancies or fluoride interstitials are close to thorium. This is expected to be the lowest-energy configuration due to electrostatic attraction between oppositely charged defects. Defect formation energies were calculated using the binary fluorides  $\text{ThF}_4$ ,  $\text{BaF}_2$ , and  $\text{MgF}_2$  as reactants and side products. Defects were studied using a  $4 \times 1 \times 3$  supercell of  $\text{BaMgF}_4$  with side lengths of approximately 15 Å. The defect formation energies are 1.30 eV for  $\text{Th}_{\text{Ba}}^{2+} + \text{V}_{\text{Mg}}^{2-}$ , 1.70 eV for  $\text{Th}_{\text{Ba}}^{2+} + \text{V}_{\text{Ba}}^{2-}$ , and 1.96 eV for  $\text{Th}_{\text{Ba}}^{2+} + 2\text{F}_i^-$ . Optimized unit cells for all three defects are shown in the supporting information, and the formation and defect energies are summarized in Table I. Due

| Defect   | $\Delta E_f$ (eV) | $E_d$ (eV) |
|--|-------------------|------------|
| $\text{Th}_{\text{Ba}}^{2+} + \text{V}_{\text{Mg}}^{2-}$ | 1.30              | 5.97       |
| $\text{Th}_{\text{Ba}}^{2+} + \text{V}_{\text{Ba}}^{2-}$ | 1.70              | 5.73       |
| $\text{Th}_{\text{Ba}}^{2+} + 2\text{F}_i^-$             | 1.96              | 6.50       |

TABLE I. Calculated formation ( $\Delta E_f$ ) and defect ( $E_d$ ) energies of thorium defects in  $\text{BaMgF}_4$ .

to the large energy gap between the magnesium vacancy and barium vacancy defects, we expect  $\text{Th}_{\text{Ba}}^{2+} + \text{V}_{\text{Mg}}^{2-}$  to be the dom-

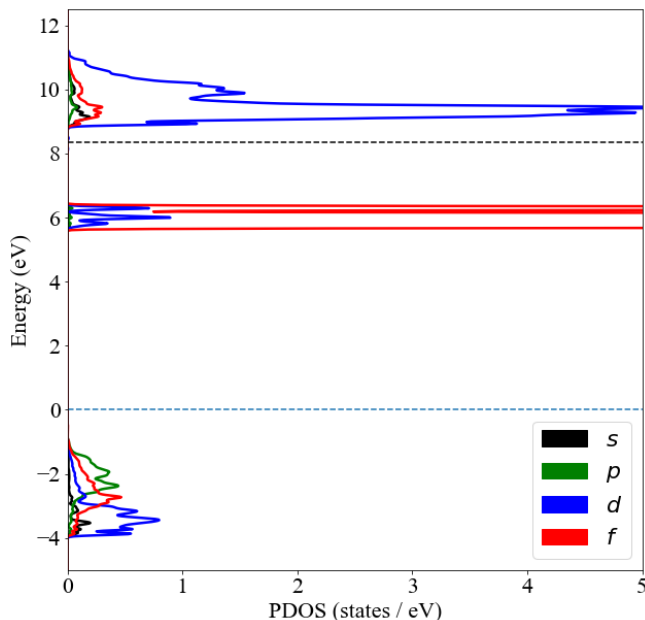


FIG. 3. Thorium PDOS for the  $\text{Th}_{\text{Ba}}^{..} + \text{V}_{\text{Mg}}^{..}$  defect in  $\text{Th}:\text{BaMgF}_4$ . The dashed black line represents the energy of the  $^{229}\text{Th}$  nuclear excited state relative to the top of the valence band.

inant thorium environment in Th-doped  $\text{BaMgF}_4$ . If thermal equilibrium were established at 1138 K, the melting point of  $\text{BaMgF}_4$ ,<sup>30</sup> then more than 98% of the thorium would be in  $\text{Th}_{\text{Ba}}^{..} + \text{V}_{\text{Mg}}^{..}$  defects; this is a lower bound on the population of the defect, so it should dominate observed properties associated with thorium<sup>31</sup>.

The thorium-projected density of states (PDOS) for the  $\text{Th}_{\text{Ba}}^{..} + \text{V}_{\text{Mg}}^{..}$  cell is shown in Figure 3. The difference in energy from the Fermi energy to the first defect electronic state,  $E_d$ , is 5.97 eV. However, the Th orbitals make no contribution to the uppermost part of the valence band, which suggests that the highest occupied states have no overlap with thorium. The Th 5*f* PDOS is non-negligible below approximately -1 eV, so the lowest-energy electronic transition where both initial and final states overlap with thorium is around 7 eV. This is likely because the occupied states at the top of the valence band are localized on fluoride ions near the magnesium vacancy that do not overlap with thorium. Above the Th 5*f* band there is a significant energy window with zero density of states before the Th 6*d* band and bulk conduction band appear at 9 eV.

The thorium PDOS for the  $\text{Th}_{\text{Ba}}^{..} + \text{V}_{\text{Ba}}^{..}$  cell is shown in Figure S2. For this configuration  $E_d=5.73$  eV, and the Th PDOS is very similar to that in the  $\text{Th}_{\text{Ba}}^{..} + \text{V}_{\text{Mg}}^{..}$  cell.

Finally, the thorium PDOS for the  $\text{Th}_{\text{Ba}}^{..} + 2\text{F}_i'$  defect is shown in Figure S3. It is broadly similar to the PDOSs of the other defects, with  $E_d=6.50$  eV. Unlike the cation vacancy cells, Th 5*f* character is present near the top of the valence band.

The PDOS of all three of these configurations are qualitatively similar to that of the lowest energy defect for  $^{229}\text{Th}:\text{LiSrAlF}_6$  ( $\text{Th}_{\text{Sr}}^{..} + 2\text{F}_i'$ )<sup>7</sup> and  $^{229}\text{Th}:\text{CaF}_2$  ( $\text{Th}_{\text{Ca}}^{..} +$

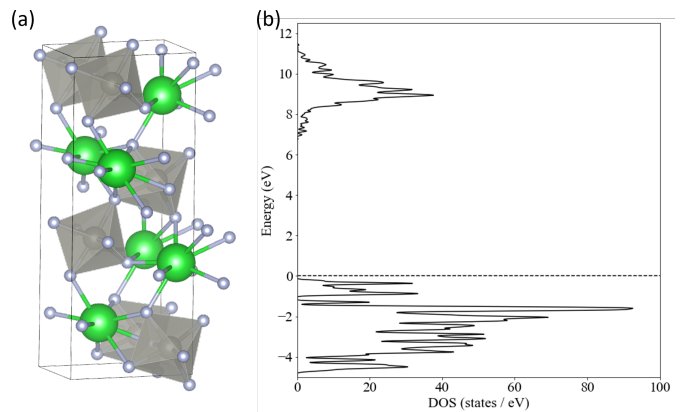


FIG. 4. (a) Unit cell of  $\text{BaZnF}_4$ . Ba is shown in green, Zn in dark grey, and F in light grey. (b) Total density of states (DOS) of  $\text{BaZnF}_4$ .

$2\text{F}_i'$ )<sup>32</sup>. Given that a narrow nuclear resonance has been seen in both of these materials,  $^{229}\text{Th}:\text{BaMgF}_4$  appears to be a promising candidate for a compact solid-state clock. However, given the difficulty in growing  $^{229}\text{Th}$ -doped materials, verification of this by successful observation of long-lived nuclear fluorescence following Ref.<sup>33</sup> would be an important next step.

## B. $\text{BaZnF}_4$

The same set of calculations was performed for  $\text{BaZnF}_4$ , which has the same structure as  $\text{BaMgF}_4$ . The optimized structure and DOS are shown in Figure 4. The computed band gap is 7.00 eV, an underestimate compared to the experimental (absorption edge) value of 8.55 eV.<sup>27</sup> Since measurements of the band gap suggest that it is in fact slightly higher than the nuclear transition energy, we analyzed the energy of Th defects in the material.

The three defect cells equivalent to those studied in  $\text{BaMgF}_4$  were constructed; Th replaces Ba in all cases, and the charge is compensated by either  $\text{V}_{\text{Ba}}^{..}$ ,  $\text{V}_{\text{Zn}}^{..}$ , or  $2\text{F}_i'$ . The calculated properties of these defects are summarized in Table II. The formation energies are all lower than their equiv-

| Defect   | $\Delta E_f$ (eV) | $E_d$ (eV) |
|--|-------------------|------------|
| $\text{Th}_{\text{Ba}}^{..} + \text{V}_{\text{Zn}}^{..}$ | 0.68              | 4.44       |
| $\text{Th}_{\text{Ba}}^{..} + \text{V}_{\text{Ba}}^{..}$ | 1.05              | 5.01       |
| $\text{Th}_{\text{Ba}}^{..} + 2\text{F}_i'$              | 1.28              | 5.36       |

TABLE II. Calculated formation energies  $\Delta E_f$  and Fermi energy to first defect state energies  $E_d$  of thorium defects in  $\text{BaZnF}_4$ .

alents in  $\text{BaMgF}_4$ , suggesting that  $\text{BaZnF}_4$  may host a higher concentration of thorium. The relative energies of the defects follow the same trend, with a  $\text{Zn}^{2+}$  vacancy being the most likely charge compensating defect, followed by a  $\text{Ba}^{2+}$  vacancy, and  $\text{F}^-$  interstitials. Thorium PDOS plots for the defect cells are shown in Figures S4-S6. They show that the electronic properties of thorium in  $\text{Th}:\text{BaZnF}_4$  are much the

same as in Th:BaMgF<sub>4</sub>. In the cation vacancy cells the Th 5*f* orbitals form narrow peaks at 4-6 eV, though the majority of the thorium-containing states in the valence band are more than 2 eV below the Fermi level so the electronic transitions involved in internal conversion may be higher energy. Nevertheless, given the clear gap between the thorium 5*f* band and the conduction band, and the fact that the experimental band gap is only just above the nuclear transition energy, we suspect that internal conversion through the Th 5*f* orbitals could be possible in Th:BaZnF<sub>4</sub>.

The difference in defect stats of BaMgF<sub>4</sub> and BaZnF<sub>4</sub> results from the valence orbitals of Mg<sup>2+</sup> and Zn<sup>2+</sup>. Zinc lies at the end of the first transition series, so Zn<sup>2+</sup> has a 3*d*<sup>10</sup>4*s*<sup>0</sup> electronic configuration. The 3*d* orbitals are chemically inert, in that there are no generally accepted reports of Zn<sup>3+</sup> compounds, but the PDOS plots in Figures S7 show that the top of the valence band is principally composed of Zn 3*d* orbitals, somewhat hybridized with F 2*p*<sup>34,35</sup>. This contrasts with the valence band in BaMgF<sub>4</sub> which is entirely F 2*p* because the highest occupied orbital in Mg<sup>2+</sup> is the core-like 2*p*. In both cases the conduction band is predominantly Ba 5*d*, though the band gap of BaZnF<sub>4</sub> may be somewhat reduced by the low-lying 4*s* orbital of Zn<sup>2+</sup>.

As a result, the two materials have fundamentally different excited electronic states. In Th:BaMgF<sub>4</sub> the first excited state is an electron transfer from F<sup>-</sup> to Th<sup>4+</sup>, similar to what is expected in other fluorides like LiSrAlF<sub>6</sub> and CaF<sub>2</sub>. However, in Th:BaZnF<sub>4</sub> the hole created by electronic excitation will be centered on zinc, likely with significant hybridization with fluorine. The different excited state characters could affect wavefunction overlap and lead to different nuclear quenching behavior in the two materials.

### C. DFT methods

DFT calculations on were performed with VASP<sup>36</sup>, version 6.4.2, using the PAW<sup>37</sup> method with a plane-wave cutoff of 500 eV and a spin-restricted formalism. The PBE<sup>38</sup> functional was used for all structural optimizations, and the modified Becke-Johnson (MBJ)<sup>28,29</sup> functional was used for electronic properties. Structural optimizations were performed using a  $\Gamma$ -centered *k*-meshes with point spacings of 8-2-6 for bulk BaMgF<sub>4</sub> and BaZnF<sub>4</sub>, and 2-2-2 for the defect supercells, all equivalent to a *k*-point spacing of 0.03 Å<sup>-1</sup>. Structural optimizations of other binary fluorides also used a *k*-point spacing of 0.03 Å<sup>-1</sup>. MBJ calculations on the bulk unit cells used 8-2-6 *k*-point grids, and MBJ calculations on the defect supercells used 3-3-3 *k*-point grids. *k*-point grids were generated with VASPKIT.<sup>39</sup>

### III. OPTICAL CONTACT BONDING

Figure 1 outlines a composite optical crystal for optical doubling and excitation of <sup>229</sup>Th. In this system the incident laser first reaches pure a nonlinear material to generate 148

nm photons. These photons then travel into a <sup>229</sup>Th-doped crystal to excite the <sup>229</sup>Th.

Clearly, this requires that the interface between the two halves of the crystal be transparent to photons. Assuming no adhesives are used to bond the crystals, they must be held together by van der Waals interactions<sup>40</sup>, a process known as ‘optical contact bonding’.

For the bonding to work the crystal surfaces must be exceptionally flat and clean. Surface preparation typically involves extensive polishing, and the actual contacting procedure may be done under vacuum. Additional processing steps can improve the quality of the contact. High pressure can be applied to try to overcome surface roughness. Annealing, where energy is supplied to the system for the atoms close to the contact to rearrange into a more stable configuration, can be done with heat, electricity, or light. A more recent development is ‘chemical activation’ of the surface. The basic principle is to disturb the surface significantly at the atomic level, creating ‘dangling bonds’ that will easily form covalent bonds between the surfaces when they are joined. This can be done by surface chemical reactions, such as hydroxy-catalysis bonding in silicate glasses, or physical processes, such as ion beam or plasma etching<sup>41,42</sup>.

Several factors indicate that bonding of a BaMgF<sub>4</sub>/Th:BaMgF<sub>4</sub> composite is likely to be successful. It involves bonding doped and undoped crystals of the same material so the lattice constants and coefficients of thermal expansion are near-perfectly matched. In a relevant study, a composite system of pure and Nb-doped YAG was successfully produced by optical contacting including surface activation by argon atom beam etching.<sup>42</sup> Fluorides can be used in optical contact bonding, including YLiF<sub>4</sub> and LuLiF<sub>4</sub>, as can non-linear optical materials<sup>43</sup>.

### IV. EXAMPLE CLOCK

As an example of a potential architecture for solid-state clock, we consider the example of BaMgF<sub>4</sub> probed with a single  $\sim 296.8$  nm laser, as shown in Fig. 1 (a). The clock transition frequency is primarily determined by the isomer shift, the crystal electric field gradient, and the local magnetic field. The isomer shift, also known as the chemical shift in Mössbauer spectroscopy, is primarily associated with the interaction between the nuclear charge distribution and the electronic environment surrounding the nucleus. As a result, the apparent nuclear transition frequency varies across different hosts and doping sites. We estimate the isomer shifts by summing over the partial density of states integrated over the valence band (IPDOS) for various partial waves (*s*, *p*, *d*, and *f*) weighted by the isomer shifts for the valence atomic states of <sup>229</sup>Th<sup>3+</sup> ion. This procedure yields isomer shifts relative to the apparent nuclear clock frequency for the <sup>229</sup>Th<sup>4+</sup> closed-shell ion. <sup>229</sup>Th<sup>4+</sup> serves as a convenient reference as its electronic cloud remains largely unperturbed by the crystal fields as supported by our density of state calculations. We find that the isomer shifts range from  $\delta_{\text{iso}} = -254$  MHz to  $-258$  MHz for BaMgF<sub>4</sub> materials and over a much wider

range,  $\delta_{\text{iso}} = -224$  MHz to  $-268$  MHz for BaZnF<sub>4</sub> due to a much larger IPDOS variations across BaZnF<sub>4</sub> substitutions. These values are for the lowest formation energy defects compiled in Tables I and II. For comparison, we find the isomer shift of <sup>229</sup>Th:LiSrAlF<sub>6</sub> and <sup>229</sup>Th:CaF<sub>2</sub> as  $-248$  MHz and  $-243$  MHz, respectively.

In addition to the isomer shift, the main effects of the crystalline host on the <sup>229</sup>Th<sup>4+</sup> nucleus are the coupling of the <sup>229</sup>Th nuclear electric quadrupole (EQ) moment to the crystal electric field gradients (EFG)  $\{V_{xx}, V_{yy}, V_{zz}\}$  and the coupling of the <sup>229</sup>Th nuclear magnetic moment to the magnetic field created by the other atoms in the crystal<sup>2</sup>. <sup>229</sup>Th:BaMgF<sub>4</sub> is an ionic crystal with no unpaired electrons and therefore the magnetic field experienced by a <sup>229</sup>Th atom comes from the other nuclear magnetic moments in the crystal. Thus, the nuclear energy levels are described by the Hamiltonian:

$$\hat{H} = -\mu_{\alpha}\vec{I}\cdot\vec{B} + \frac{eQ_{\alpha}V_{zz}}{4I(2I-1)} [3\hat{I}_z^2 - \hat{I}^2 + \eta(\hat{I}_x^2 - \hat{I}_y^2)],$$

where  $\hat{I}$  is the total nuclear spin operator,  $\hat{I}_{x,y,z}$  are the component of the nuclear spin operators,  $\eta = |V_{xx} - V_{yy}|/V_{zz}$  is the EFG asymmetry parameter with the choice  $|V_{zz}| > |V_{xx}| > |V_{yy}|$ , and  $\alpha = \{g, e\}$  denotes the ground and excited nuclear states, respectively, which is parameterized by  $Q_g = 3.149(4)$  eb<sup>44</sup>,  $\mu_g = 0.360(7)\mu_N$ <sup>45,46</sup>,  $Q_e = 1.77(2)$  eb<sup>47,48</sup>, and  $\mu_e = -0.378(8)\mu_N$ <sup>47,48</sup>, where  $\mu_N$  is the nuclear magneton. The DFT calculations described above predict  $V_{zz} = 398$  V/Å<sup>2</sup> and  $\eta = 0.585$ , leading to the splitting of the nuclear levels as shown in Fig. 5. Using the DFT predicted positions of the F atoms in the BaMgF<sub>4</sub> crystal, we find that fluctuations in the magnetic field at the position of the <sup>229</sup>Th nucleus leads to an inhomogenous broadening of the  $|I = 5/2, m_I = \pm 1/2\rangle \leftrightarrow |3/2, \pm 1/2\rangle$  transition of  $\approx 700$  Hz. Based on the measurement in Ref.<sup>49</sup>, we predict this transition occurs at approximately 2020407371(2) MHz.

To produce light at this frequency, we assume efficient frequency doubling requires quasi-phase matching in the BaMgF<sub>4</sub> crystal. Given that the largest nonlinear doubling coefficient is  $d_{32} \sim 0.06$  pm/V<sup>20</sup>, we take the input polarization along the crystal *b*-axis. From the Sellmeier coefficients provided in<sup>20</sup>, the indices of refraction are estimated as 1.645 at 148.4 nm, and 1.472 at 296.8 nm. This yields a poling period of  $\Lambda = 2\pi/\Delta k \approx 858$  nm. Sub-micron poling has been demonstrated in lithium niobate thin films<sup>50</sup>, however, to our knowledge it has not been extended to bulk crystals. As such, we consider the doubling efficiency based on both a  $\Lambda$ - and  $3\Lambda$ -poled crystal.

The intensity  $I_2$  of second-harmonic radiation generated in a doubling crystal with  $m\Lambda$ -poling is given by<sup>51</sup>

$$I_2(2\omega) = \frac{2d_m^2(2\omega)^2 I_1^2}{n_1^2 n_2 \epsilon_0 c^3} L^2, \quad (1)$$

where

$$d_m = \frac{2d_{32}}{\pi m}. \quad (2)$$

If we assume  $I_1 = 200$  mW/mm<sup>2</sup> of 296.8 nm light into a  $L = 5$  mm BaMgF<sub>4</sub> crystal one will obtain  $5.5 \times 10^{-7}$  mW/mm<sup>2</sup> of

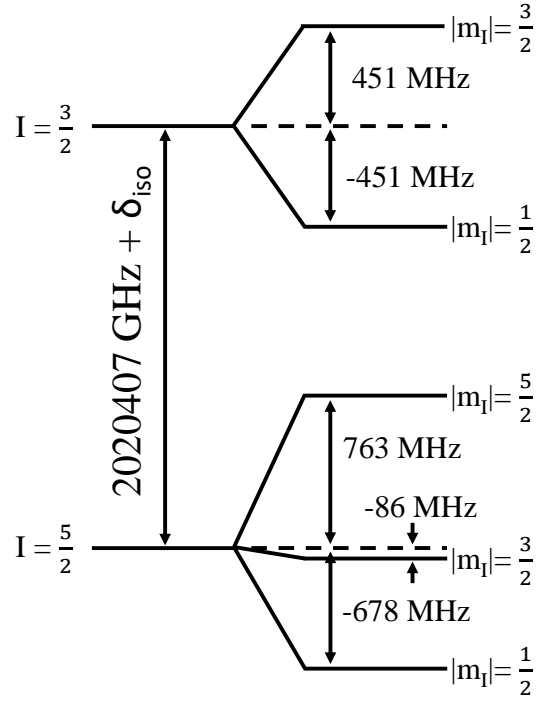


FIG. 5. Splitting of the  $|m_I\rangle$  levels of the nuclear ground and isomeric state in the electric field gradient of BaMgF<sub>4</sub>.

148.4 nm light for  $\Lambda$ -poling and  $6.1 \times 10^{-8}$  mW/mm<sup>2</sup> for  $3\Lambda$ -poling. For the remaining analysis the input light is assumed to have a 1 kHz linewidth.

Assuming that the generated light enters a 1 cm BaMgF<sub>4</sub> region doped with <sup>229</sup>Th at a doping density of  $10^{16}$  cm<sup>-3</sup>, the ultimate limit on the clock stability is given by<sup>52</sup>

$$\sigma = \frac{1}{2\pi QS} \sqrt{\frac{T_e + T_c}{\tau}}, \quad (3)$$

where  $Q = f_0/\Delta f$  is the transition quality factor,  $S$  is the signal-to-noise ratio (SNR),  $T_e$  is the excitation time,  $T_c$  is the fluorescence collection time, and  $\tau$  is the averaging time. The SNR is given by  $S = \frac{N_d}{\sqrt{N_d + b \times T_c}}$ , where  $b = 200$  cps based on backgrounds measured in <sup>229</sup>Th:LiSrAlF<sub>6</sub> crystals, and  $N_d$  is the number of detected photons given by  $N_d = \eta N_e (1 - e^{-\Gamma T_c})$ , where  $N_e$  the total number of <sup>229</sup>Th nuclei excited,  $\eta = 0.01$  is the assumed system detection efficiency, and  $\Gamma$  is the transition decay rate. Optimizing  $\sigma$  with respect to  $(T_e, T_c)$ , we find the ideal combinations as (570 s, 570 s) for  $\Lambda$  and (580 s, 550 s) for  $3\Lambda$ . From the assumed parameters we obtain a projected clock performance of  $5 \times 10^{-16}/\sqrt{\tau}$  and  $2 \times 10^{-15}/\sqrt{\tau}$  for  $\Lambda$  and  $3\Lambda$ -poling, respectively.

## V. CONCLUSION

In order to advance the development of a solid-state nuclear clock, we analyzed the viability of BaMgF<sub>4</sub> and BaZnF<sub>4</sub> for generating VUV radiation at the <sup>229</sup>Th isomer wavelength of

148.6 nm. In addition, we propose to directly dope  $^{229}\text{Th}$  into a VUV doubling crystal as a potential “vacuum-free” VUV laser clock or to join the VUV doubling and  $^{229}\text{Th}$ -doped crystal together through optical contacting. In line with the former proposal, we have analyzed the potential shifts and broadenings that the crystalline environments could introduce to the isomeric transition, and have estimated the clock performance of an all-BaMgF<sub>4</sub> nuclear clock.

## ACKNOWLEDGMENTS

This work was supported by NSF awards PHYS-2013011, PHY-2207546, and PHYS-2412982, and ARO award W911NF-11-1-0369. ERH acknowledges institutional support by the NSF QLCI Award OMA-2016245. This work used Bridges-2 at Pittsburgh Supercomputing Center through allocation PHY230110 from the Advanced Cyberinfrastructure Coordination Ecosystem: Services & Support (ACCESS) program, which is supported by National Science Foundation grants #2138259, #2138286, #2138307, #2137603, and #2138296.

## DATA AVAILABILITY STATEMENT

The data that support the findings of this study are available within the article [and its supplementary material].

- <sup>1</sup>E. R. Hudson, A. C. Vutha, S. K. Lamoreaux, and D. DeMille, “Investigation of the optical transition in the  $^{229}\text{Th}$  nucleus: Solid-state optical frequency standard and fundamental constant variation,” *Int. Conf. Atm. Phys.*, poster M028 (2008).
- <sup>2</sup>W. G. Rellergert, D. DeMille, R. R. Greco, M. P. Hehlen, J. R. Torgerson, and E. R. Hudson, “Constraining the evolution of the fundamental constants with a solid-state optical frequency reference based on the  $^{229}\text{Th}$  nucleus,” *Physical Review Letters* **104**, 200802 (2010).
- <sup>3</sup>W. G. Rellergert, D. DeMille, R. R. Greco, M. P. Hehlen, J. R. Torgerson, and E. R. Hudson, “Constraining the evolution of the fundamental constants with a solid-state optical frequency reference based on the  $^{229}\text{Th}$  nucleus,” *Physical Review Letters* **104**, 200802 (2010).
- <sup>4</sup>E. V. Tkalya, “Proposal for a Nuclear Gamma-Ray Laser of Optical Range,” *Physical Review Letters* **106**, 162501 (2011), arXiv:1011.0858 [nucl-th].
- <sup>5</sup>E. Peik, T. Schumm, M. S. Safronova, A. Pálffy, J. Weitenberg, and P. G. Thirolf, “Nuclear clocks for testing fundamental physics,” *Quantum Science and Technology* **6**, 034002 (2021).
- <sup>6</sup>P. Gütllich, C. Schröder, and V. Schünemann, “Mössbauer spectroscopy—an indispensable tool in solid state research,” *Spectroscopy Europe/World* **24**, 21–31 (2012).
- <sup>7</sup>R. Elwell, C. Schneider, J. Jeet, J. E. S. Terhune, H. W. T. Morgan, A. N. Alexandrova, H. B. Tran Tan, A. Derevianko, and E. R. Hudson, “Laser excitation of the  $^{229}\text{Th}$  nuclear isomeric transition in a solid-state host,” *Physical Review Letters* **133**, 013201 (2024).
- <sup>8</sup>L. Kroger and C. Reich, “Features of the low-energy level scheme of  $^{229}\text{Th}$  as observed in the  $\alpha$ -decay of  $^{233}\text{U}$ ,” *Nuclear Physics A* **259**, 29–60 (1976).
- <sup>9</sup>R. G. Helmer and C. W. Reich, “An excited state of  $^{229}\text{Th}$  at 3.5 eV,” *Physical Review C* **49**, 1845–1858 (1994).
- <sup>10</sup>S. B. Utter, P. Beiersdorfer, A. Barnes, R. W. Loughheed, J. R. Crespo López-Urrutia, J. A. Becker, and M. S. Weiss, “Reexamination of the optical gamma ray decay in  $^{229}\text{Th}$ ,” *Physical Review Letters* **82**, 505–508 (1999).
- <sup>11</sup>R. W. Shaw, J. P. Young, S. P. Cooper, and O. F. Webb, “Spontaneous ultraviolet emission from  $^{233}\text{Uranium}/^{229}\text{Thorium}$  samples,” *Physical Review Letters* **82**, 1109–1111 (1999).
- <sup>12</sup>B. R. Beck, J. A. Becker, P. Beiersdorfer, G. V. Brown, K. J. Moody, J. B. Wilhelmy, F. S. Porter, C. A. Kilbourne, and R. L. Kelley, “Energy splitting of the ground-state doublet in the nucleus  $^{229}\text{Th}$ ,” *Physical Review Letters* **98**, 142501 (2007).
- <sup>13</sup>B. R. Beck, C. Y. Wu, P. Beiersdorfer, G. V. Brown, J. A. Becker, J. K. Moody, J. B. Wilhelmy, F. S. Porter, C. A. Kilbourne, and R. L. Kelley, “Improved value for the energy splitting of the ground-state doublet in the nucleus  $^{229}\text{Th}$ ,” Conference LLNL-PROC-415170 (Lawrence Livermore National Laboratory, Livermore, CA, 2009).
- <sup>14</sup>J. Tiedau, M. V. Okhapkin, K. Zhang, J. Thielking, G. Zitzler, E. Peik, F. Schaden, T. Pronebner, I. Morawetz, L. Toscani De Col, *et al.*, “Laser excitation of the Th-229 nucleus,” *Physical Review Letters* **132**, 182501 (2024).
- <sup>15</sup>E.R. Hudson, U.S. Provisional Patent Application No. 63/670,220 (2024).
- <sup>16</sup>T. Nakazato, I. Ito, Y. Kobayashi, X. Wang, C. Chen, and S. Watanabe, “Phase-matched frequency conversion below 150 nm in KBe<sub>2</sub>BO<sub>3</sub>F<sub>2</sub>,” *Optics Express* **24**, 17149–17158 (2016).
- <sup>17</sup>D. N. Nikogosyan, “Beta barium borate (BBO),” *Applied Physics A* **52**, 359–368 (1991).
- <sup>18</sup>L. Kang and Z. Lin, “Deep-ultraviolet nonlinear optical crystals: concept development and materials discovery,” *Light: Science & Applications* **11**, 201 (2022).
- <sup>19</sup>G. Peng *et al.*, “NH<sub>4</sub>Be<sub>2</sub>BO<sub>3</sub>F<sub>2</sub> and g-Be<sub>2</sub>BO<sub>3</sub>F: Overcoming the layering habit in KBe<sub>2</sub>BO<sub>3</sub>F<sub>2</sub> for the next-generation deep-ultraviolet nonlinear optical materials,” *Angewandte Chemie* **57**, 8968 (2018).
- <sup>20</sup>S. Buchter, Y. Fan, V. Liberman, J. Zayhowski, M. Rothschild, E. Mason, A. Cassanho, H. Jenssen, and J. Burnett, “Periodically poled BaMgF<sub>4</sub> for ultraviolet frequency generation,” *Optics Letters* **26**, 1693 (2001).
- <sup>21</sup>S. Herr, H. Tanaka, I. Breunig, M. Bickermann, and F. Kuknemann, “Fanout periodic poling of BaMgF<sub>4</sub> crystals,” *Optical Materials Express* **13**, 2158 (2023).
- <sup>22</sup>E. Villora, K. Shimamura, F. Jing, A. Medvedev, S. Takekawa, and K. Kitamura, “Ferroelectric and optical properties of single crystal BaZnF<sub>4</sub>,” *Applied Physics Letters* **90**, 192909 (2007).
- <sup>23</sup>J. Ellis, X. Wen, and R. Martin, “Investigation of thorium salts as candidate materials for direct observation of the  $^{229}\text{Th}$  nuclear transition,” *Inorganic Chemistry* **53**, 6769–6774 (2014).
- <sup>24</sup>M. Pimon, J. Gugler, P. Mohn, G. A. Kazakov, N. Mauser, and T. Schumm, “DFT calculation of (229)thorium-doped magnesium fluoride for nuclear laser spectroscopy,” *Journal of Physics-Condensed Matter* **32** (2020), 10.1088/1361-648X/ab7c90.
- <sup>25</sup>M. Pimon, P. Mohn, and T. Schumm, “Band gap calculations for thorium-doped LiCAF,” *Advanced Theory and Simulations* **5** (2022), 10.1002/adts.202200185.
- <sup>26</sup>F. Gingl, “BaMgF<sub>4</sub> and Ba<sub>2</sub>Mg<sub>3</sub>F<sub>10</sub>: New examples for structural relationships between hydrides and fluorides,” *Zeitschrift für Anorganische und Allgemeine Chemie* **623**, 705–709 (1997).
- <sup>27</sup>E. Villora, K. Shimamura, F. Jing, A. Medvedev, S. Takekawa, and K. Kitamura, “Ferroelectric and optical properties of single crystal BaZnF<sub>4</sub>,” *Applied Physics Letters* **90** (2007), 10.1063/1.2737365.
- <sup>28</sup>F. Tran and P. Blaha, “Accurate band gaps of semiconductors and insulators with a semilocal exchange-correlation potential,” *Physical Review Letters* **102** (2009), 10.1103/PhysRevLett.102.226401.
- <sup>29</sup>A. D. Becke and E. R. Johnson, “A simple effective potential for exchange,” *Journal of Chemical Physics* **124** (2006), 10.1063/1.2213970.
- <sup>30</sup>T. Pollak, “Crystal growth and characterization of BaMgF<sub>4</sub>,” <https://apps.dtic.mil/sti/citations/ADA146805> (1984), [Accessed 21-10-2024].
- <sup>31</sup>G. Vineyard and G. Dienes, “The theory of defect concentration in crystals,” *Physical Review* **93**, 265–268 (1954).
- <sup>32</sup>B. S. Nickerson, *Towards coherent control of the  $^{229}\text{Th}$  isomeric transition in VUV-transparent crystals*, Ph.D. thesis, Ruperto-Carola-University of Heidelberg (2019).
- <sup>33</sup>S. V. Pineda, P. Chhetri, S. Bara, Y. Elskens, S. Casci, A. N. Alexandrova, M. Au, M. Athanasakis-Kaklamanakis, M. Bartokos, K. Beeks, C. Berner, A. Claessens, K. Chrysalidis, T. E. Cocolios, J. G. Correia, H. D. Witte, R. Elwell, R. Ferrer, R. Heinke, E. R. Hudson, F. Ivandikov, Y. Kudryavtsev, U. Köster, S. Kraemer, M. Laatiaoui, R. Lica, C. Merckling, I. Morawetz, H. W. T. Morgan, D. Moritz, L. M. C. Pereira, S. Raeder, S. Rothe, F. Schaden, K. Scharl, T. Schumm, S. Stegemann, J. Terhune,

- P. G. Thirof, S. M. Tunhuma, P. V. D. Bergh, P. V. Duppen, A. Vantomme, U. Wahl, and Z. Yue, "Radiative decay of the  $^{229m}\text{Th}$  nuclear clock isomer in different host materials," (2024), [arXiv:2408.12309 \[nucl-ex\]](https://arxiv.org/abs/2408.12309).
- <sup>34</sup>Y. Shang, N. Shu, Z. Zhang, P. Yang, and J. Xu, "Comment on "realization of the  $\text{Zn}^{3+}$  oxidation state" by H. Fang, H. Banjade, Deepika and P. Jena," *Nanoscale* **14**, 8875–8880 (2022).
- <sup>35</sup>T. Schlöder, M. Kaupp, and S. Riedel, "Can zinc really exist in its oxidation state plus III?" *Journal of the American Chemical Society* **134**, 11977–11979 (2012).
- <sup>36</sup>G. Kresse and J. Furthmüller, "Efficient iterative schemes for ab initio total-energy calculations using a plane-wave basis set," *Physical Review B* **54**, 11169–11186 (1996).
- <sup>37</sup>P. E. Blochl, "Projector augmented wave method," *Physical Review B* **50**, 17953–17979 (1994).
- <sup>38</sup>J. P. Perdew, K. Burke, and M. Ernzerhof, "Generalized gradient approximation made simple," *Physical Review Letters* **77**, 3865–3868 (1996).
- <sup>39</sup>V. Wang, N. Xu, J.-C. Liu, G. Tang, and W.-T. Geng, "Vaspkit: A user-friendly interface facilitating high-throughput computing and analysis using vasp code," *Computer Physics Communications* **267**, 108033 (2021).
- <sup>40</sup>J. Haisma and G. Spierings, "Contact bonding, including direct-bonding in a historical and recent context of materials science and technology, physics and chemistry - historical review in a broader scope and comparative outlook," *Materials Science and Engineering R-Reports* **37**, 1–60 (2002).
- <sup>41</sup>K. Green, J. Burke, and B. Oreb, "Chemical bonding of ultra low expansion glass substrates with aqueous NaOH solution," *Materials Chemistry and Physics* **130**, 577–582 (2011).
- <sup>42</sup>K. Fujioka, A. Sugiyama, Y. Fujimoto, J. Kawanaka, and N. Miyanaga, "Ion diffusion at the bonding interface of undoped YAG/Yb:YAG composite ceramics," *Optical Materials* **46**, 542–547 (2015).
- <sup>43</sup>"Material combinations - onysoptics.com," <http://www.onysoptics.com/material-combinations.html>, [Accessed 21-10-2024].
- <sup>44</sup>C. E. Bemis, F. K. McGowan, J. L. C. Ford, Jr., W. T. Milner, R. L. Robinson, P. H. Stelson, G. A. Leander, and C. W. Reich, "Coulomb excitation of states in  $^{229}\text{Th}$ ," *Phys. Scr.* **38**, 657–663 (1988).
- <sup>45</sup>S. Gerstenkorn, P. Luc, J. Verges, D. Englekemeir, J. Gindler, and F. Tomkins, "Structures hyperfines du spectre d'étincelle, moment magnétique et quadrupolaire de l'isotope 229 du thorium," *Journal de Physique* **35**, 483–495 (1974).
- <sup>46</sup>C. Campbell, A. Radnaev, and A. Kuzmich, "Wigner Crystals of  $^{229}\text{Th}$  for Optical Excitation of the Nuclear Isomer," *Physical Review Letters*. **106**, 223001 (2011).
- <sup>47</sup>J. Thielking, M. V. Okhupkin, P. Glowacki, D. M. Meier, L. von der Wense, B. Seiferle, C. E. Düllmann, P. G. Thirof, and E. Peik, "Laser spectroscopic characterization of the nuclear-clock isomer  $^{229m}\text{Th}$ ," *Nature* **556**, 321–325 (2018).
- <sup>48</sup>A. Yamaguchi, Y. Shigekawa, H. Haba, H. Kikunaga, K. Shirasaki, M. Wada, and H. Katori, "Laser spectroscopy of triply charged  $^{229}\text{Th}$  isomer for a nuclear clock," *Nature* **629**, 62–66 (2024).
- <sup>49</sup>C. Zhang, T. Ooi, J. S. Higgins, J. F. Doyle, L. von der Wense, K. Beeks, A. Leitner, G. A. Kazakov, P. Li, P. G. Thirof, T. Schumm, and J. Ye, "Frequency ratio of the  $^{229m}\text{Th}$  nuclear isomeric transition and the  $^{87}\text{Sr}$  atomic clock," *Nature* **633**, 63–70 (2024).
- <sup>50</sup>B. Slautin, H. Zhu, and V. Y. Shur, "Submicron periodical poling by local switching in ion sliced lithium niobate thin films with a dielectric layer," *Ceramics International* **47**, 32900–32904 (2021).
- <sup>51</sup>R. Boyd, *Nonlinear Optics 4th Edition* (Elsevier, 2020).
- <sup>52</sup>M. M. Boyd, *High Precision Spectroscopy of Strontium in an Optical Lattice: Towards a New Standard for Frequency and Time*, Ph.D. thesis, University of Colorado, Boulder (2007).